

## MODELING OF CENTRIFUGAL DEPLOYMENT OF THREE-SECTION MINISATELLITE BOOM

<sup>1</sup>*Institute of Technical Mechanics of the National Academy of Sciences of Ukraine and the State Space Agency of Ukraine, 15 Leshko-Popel St., Dnipro 49005, Ukraine; e-mail: skh@ukr.net*

<sup>2</sup>*Earth Observing System Data Analytics, 1906 El Camino Real, Suite 201, Menlo Park, CA 94027, USA; e-mail: vladimir.vasiliev@eos.com*

( ) .

( )

MC,

The aim of the article is to model the processes of centrifugal deployment of a three-section boom and preliminary analyze the feasibility of this deployment method for an Earth remote sensing (ERS) minisatellite (MS).

During the research, the methods of theoretical mechanics, multibody dynamics, control theory, and computer modeling were used.

Centrifugal deployment of multi-section booms have been successfully used on spin stabilized satellites, but not on ERS satellites, which have other features of operation and require additional studies.

The main part of the MS is a platform to which a transformable antenna is attached by means of a transformable boom. Before deployment, the stowed boom and antenna are attached to the MS platform. The boom sections are connected by joints with one rotational degree of freedom and deployed sequentially due to centrifugal forces when the MS rotates in the required direction. Each of the boom joints has a locking mechanism that latches when a predetermined deploy angle is reached.

To model the processes of the boom deployment, the MS is presented as a system of connected bodies, where the platform and the stowed antenna are absolutely rigid bodies, and the boom consists of three flexible beams of a tubular cross-section. The differential equations of the MS dynamics during the deployment are obtained using the Lagrangian formalism, which are supplemented by algebraic equations describing the constraints from the joints.

The scenarios of the boom deployment with a constant control torque and a constant angular velocity of the MS are considered. These scenarios are simulated and estimates of the control actions needed to ensure full deployment of the boom and the stabilization of the MS after latching of the joints are calculated. Dependences of variations of the loads on the boom structure during deployment are obtained.

The simulation results allow us to conclude that it is feasible to implement the method of the boom centrifugal deployment for the MS, which can perform fast rotations about the three axes of the body reference frame. Implementation of this method allows designers to reduce mass of the MS, because it does not require any servo drives in the boom deployment system.

**Keywords:** minisatellite, boom, centrifugal deployment, fast rotation, revolute joint, multibody dynamics.

**Introduction.** Spacecraft (SC) structure can include various attached elements of large size, such as solar panels, antennas, booms, etc. [1]. The limited space under the fairing of the launch vehicle leads to the need for such elements to be transformable, which allows them to be put into orbit in a stowed state, and then to deploy the structure into an operational state. Deployment of transformable structures in outer space is not an easy task, since it is often necessary to meet high requirements for performance and reliability under restrictions on weight, energy consumption, and others. In this regard, the processes of deployment of transformable structures are of considerable interest to scientists. For example, papers [2-7] are devoted to modeling of antenna deployment. The results of solving various problems arising in the development of transformable booms are presented in publications [8 – 11].

Despite the fact that earlier most projects with transformable structures required large satellites, nowadays, small satellites are used more and more. One such example is the minisatellite (MS) with synthetic aperture radar (SAR) [12]. Low-cost small satellite systems have the potential to expand the range of SAR applications and make them more commercially attractive.

To develop an MS with the SAR, it necessary to use approaches and solutions that differ from those conventionally used for large spacecraft. One of these promising approaches is to use a deployable reflector antenna (DRA), positioned using a transformable boom, instead of a traditional antenna with a phased array antenna [13]. In this case, it is of interest to consider the possibility of reducing the weight of the boom by not using servo drives in the deployment system. An example of such a design is a carbon fiber-reinforced polymer boom with a special cross-section. This technology makes it possible to wind the boom like a tape on a drum, and after launching the spacecraft, due to internal prestressing, to unwind it and form a sufficiently rigid rectilinear structure [14]. However, it seems problematic to meet the stringent requirements for the positioning accuracy of the DRA relative to the feedhorns using this technology. More promising design is a multisection boom made of carbon-fiber tubes. The deployment of this structure is driven by centrifugal forces during the rotation of the spacecraft [15]. Currently, there is a successful orbital experience in using such booms for spacecraft stabilized by rotation [16]. Nevertheless, due to the fact that the features of the functioning of such satellites significantly differ from the Earth remote sensing MS, it is of interest to study the feasibility of using centrifugal deployment for this class of satellites.

The aim of the article is to model the processes of centrifugal deployment of a three-section boom and preliminary analyze the feasibility of using this deployment method for an Earth remote sensing MS.

**System description and problem statement.** The MS includes a platform to which a transformable antenna is attached by means of a transformable boom (Fig. 1). Before deployment, the boom and antenna are fixed to the MS body in the stowed state (Fig. 1a).

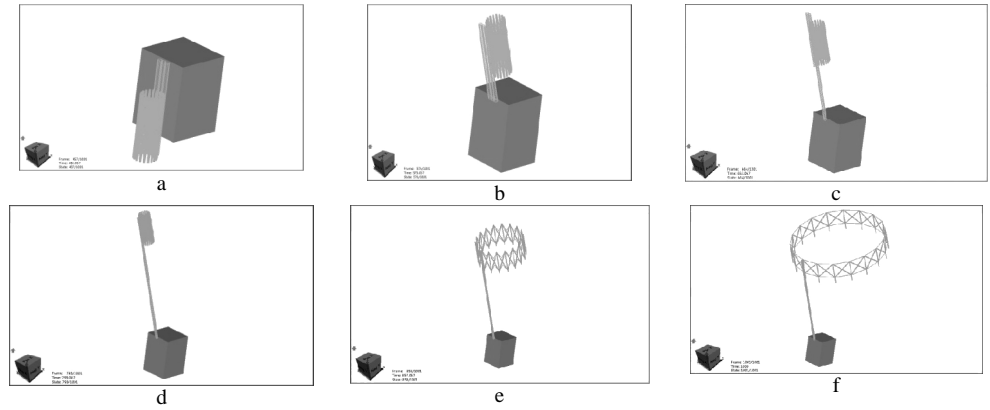


Fig. 1 – Stages of appendage deployment

The boom sections are connected by joints with one rotational degree of freedom. Each of the boom joints has a locking mechanism that latches when a predetermined deployment angle is reached. The boom sections deploy sequentially by centrifugal forces when MS rotates in the required direction (Fig. 3b-3d). After completion of the boom deployment, the deployment of the reflector begins, which is not studied in this article.

To come to a conclusion about the feasibility of this method of deployment, it is necessary to solve the following tasks:

- to build a mathematical model for modeling the centrifugal deployment of the boom;
- to simulate of the boom deployment processes and estimate the necessary control actions and the loads acting on the structure.

These tasks are investigated in this article.

**Mathematical model.** To simulate the processes of the boom deployment, the

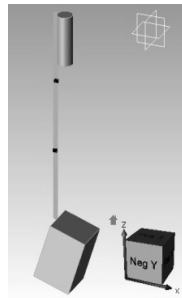


Fig. 2 – Mechanical model of the MS

MS is represented in the form of a multibody system (Fig. 2). The MS platform and the stowed antenna are modeled by absolutely rigid bodies, and the boom is modeled by three flexible beams with a tubular section. The antenna is attached to the boom using a fixed joint. The joints allowing one rotational degree of freedom are used to connect the boom sections to each other, as well as to attach it to the MS platform.

The following coordinate frames were used to describe dynamics of the MS:

$O_I x_I y_I z_I$  is the inertial coordinate frame (ICF) with the origin at the center of mass of the Earth  $O_I$ , the axis  $O_I y_I$  is directed along the rotation axis of the Earth, and the axis  $O_I z_I$  is pointed to the vernal equinox at a given epoch;

$O_S^j x_S^j y_S^j z_S^j$  are the coordinate frames fixed with the bodies (BCFs) with the origins at their centers of mass and axes coinciding with the central axes of inertia of the corresponding bodies. Hereinafter, the superscript  $j$  denotes the body number in the following sequence: 1 – MS platform; 2...4 – boom sections; 5 – antenna.

$O_S x_O y_O z_O$  is the orbital reference frame (ORF) with the origin at the center of mass of the MS, the axis  $O_S z_O$  is directed along the position vector of the center of mass of the MS relative to the center of the Earth, the axis  $O_S y_O$  is pointed along the vector of the angular momentum of the orbital motion of the MS.

Rotation matrix  $T_{IO}$  from the IRF to ORF can be given as:

$$T_{IO} = T_u T_i T_\Omega,$$

$$T_i = \begin{bmatrix} ci & si & 0 \\ -si & ci & 0 \\ 0 & 0 & 1 \end{bmatrix}, T_\Omega = \begin{bmatrix} c\Omega & 0 & -s\Omega \\ 0 & 1 & 0 \\ s\Omega & 0 & c\Omega \end{bmatrix}, T_u = \begin{bmatrix} cu & 0 & -su \\ 0 & 1 & 0 \\ su & 0 & cu \end{bmatrix},$$

where  $\Omega$  is the longitude of the ascending node,  $i$  is the inclination of the orbit,  $u$  is the argument of latitude, hereafter the symbols  $c$  and  $s$  denote in the transition matrices cos and sin, respectively.

The position of the BRF axes relative to the ORF is determined by three Euler angles: yaw  $\psi^j$ , pitch  $\varphi^j$ , roll  $\vartheta^j$ . The rotation matrix from the ORF to BRFs has the following form:

$$T_{OS}^j = T_\psi^j T_\varphi^j T_\vartheta^j,$$

where

$$T_\psi^j = \begin{bmatrix} 1 & 0 & 0 \\ 0 & c\psi^j & s\psi^j \\ 0 & -s\psi^j & c\psi^j \end{bmatrix}, T_\varphi^j = \begin{bmatrix} c\varphi^j & 0 & -s\varphi^j \\ 0 & 1 & 0 \\ s\varphi^j & 0 & c\varphi^j \end{bmatrix}, T_\vartheta^j = \begin{bmatrix} c\vartheta^j & s\vartheta^j & 0 \\ -s\vartheta^j & c\vartheta^j & 0 \\ 0 & 0 & 1 \end{bmatrix}.$$

Euler angles are convenient for understanding the attitude maneuvers of the MS, but it is known that the kinematic equations for these parameters have singular states. In this regard, a vector composed of quaternion components  $\mathbf{Q}^j = \begin{bmatrix} q_0^j \\ q_1^j \\ q_2^j \\ q_3^j \end{bmatrix}$  was used to determine the orientation of the BRFs relative to the ORF for modeling MS dynamics and control design.

The quaternion components  $\mathbf{Q}^j$  are expressed in terms of the Euler angles as follows:

$$\begin{aligned} q_0^j &= c(\vartheta^j/2)c(\varphi^j/2)c(\psi^j/2) + s(\vartheta^j/2)s(\varphi^j/2)s(\psi^j/2), \\ q_1^j &= c(\vartheta^j/2)c(\varphi^j/2)s(\psi^j/2) - s(\vartheta^j/2)s(\varphi^j/2)c(\psi^j/2), \\ q_2^j &= c(\vartheta^j/2)s(\varphi^j/2)c(\psi^j/2) + s(\vartheta^j/2)c(\varphi^j/2)s(\psi^j/2), \\ q_3^j &= s(\vartheta^j/2)c(\varphi^j/2)c(\psi^j/2) - c(\vartheta^j/2)s(\varphi^j/2)s(\psi^j/2). \end{aligned}$$

The relation between the quaternion derivative and the angular velocity with respect to the ORF  $\tilde{\omega}^j$  can be expressed as follows:

$$\dot{\mathbf{Q}}^j = 0.5 \begin{bmatrix} 0 & (-\tilde{\omega}^j)^T \\ \tilde{\omega}^j & (-\tilde{\omega}^j)^\times \end{bmatrix} \mathbf{Q}^j.$$

$$\text{where } (\tilde{\omega}^j)^{\times} = \begin{bmatrix} \mathbf{0} & -\tilde{\omega}_3^{\times} & \tilde{\omega}_2^{\times} \\ \tilde{\omega}_3^{\times} & \mathbf{0} & -\tilde{\omega}_1^{\times} \\ -\tilde{\omega}_2^{\times} & \tilde{\omega}_1^{\times} & \mathbf{0} \end{bmatrix}.$$

The displacements of the  $i$ -th node of the flexible bodies as a result of their deformations are determined as follows:

$$\dot{\mathbf{j}}_i^j = \Psi_i^j \dot{\mathbf{Y}}^j, \quad (1)$$

where  $\Psi_i^j$  is the shape matrix of natural vibration for the  $i$ -th node of the flexible body;  $\mathbf{Y}^j$  is the vector of modal coordinates.

The position of the  $i$ -th node of the flexible body in the IRF is determined as follows:

$$\mathbf{P}_i^j = \mathbf{X}_o^j + \mathbf{T}_{SI}^j \begin{pmatrix} \mathbf{j}_i^j \\ \dot{\mathbf{j}}_i^j \end{pmatrix}, \quad (2)$$

where  $\mathbf{X}_o^j$  is the position vector of the center of mass of the flexible body in the IRF;  $\mathbf{j}_i^j$  is the position vector of the  $i$ -th node in the BRF;  $\mathbf{T}_{SI}^j = (\mathbf{T}_{IO}^j)^T (\mathbf{T}_{OS}^j)^T$  is the rotation matrix from the BRF to IRF.

Joints are used to connect two bodies. The position of the joint nodes is characterized using two reference frames. We will conventionally call them action (ARF) and base (BRF) reference frames.

The fixed joint constrains three translational and rotational degrees of freedom of one body relative to another, therefore, the position and orientation of the ARF must be fixed relative to the BRF. These constrains can be described as follows:

$$\Phi_T = \mathbf{r}_a - \mathbf{r}_b = \mathbf{0}, \quad \Phi_R = \begin{bmatrix} \mathbf{g}_b^T \mathbf{h}_a \\ \mathbf{h}_b^T \mathbf{f}_a \\ \mathbf{f}_b^T \mathbf{g}_a \end{bmatrix} = \mathbf{0}, \quad (3)$$

where  $\mathbf{r}_a$ ,  $\mathbf{r}_b$  are the vectors of the absolute displacements of the ARF and BRF, respectively;  $\mathbf{f}_a$ ,  $\mathbf{g}_a$ ,  $\mathbf{h}_a$  are the vectors of the  $x$ ,  $y$ ,  $z$  axes of the ARF;  $\mathbf{f}_b$ ,  $\mathbf{g}_b$ ,  $\mathbf{h}_b$  the vectors of the  $x$ ,  $y$ ,  $z$  axes of the BRF.

The constraint force and torque are determined using Lagrange multipliers:

$$\begin{bmatrix} \mathbf{F}_a \\ \mathbf{T}_a \end{bmatrix} = \begin{bmatrix} \lambda_T \\ \lambda_R \end{bmatrix}. \quad (4)$$

The revolute joint constrains three translational and two rotational degrees of freedom. In this regard, the constraints on the translational degrees of freedom have the same form as the fixed joint, and the constraints on the rotational degrees of freedom relative to the  $x$  and  $y$  axes are given as follows:

$$\Phi_R = \begin{bmatrix} \mathbf{h}_b^T \mathbf{f}_a \\ \mathbf{h}_b^T \mathbf{g}_a \end{bmatrix} = \mathbf{0}. \quad (5)$$

The constraint torque is determined using Lagrange multipliers as follows:

$$T_a = \lambda_R + A_b \begin{bmatrix} 0 \\ 0 \\ \lambda_D + \lambda_F \end{bmatrix}, \quad (6)$$

where  $A_b$  is the matrix of the BRF orientation;  $\lambda_D$  is the torque required to rotate the joint;  $\lambda_F$  is the friction torque.

Considering the following state vector  $\mathbf{X} = [R^1, \dots, R^5, Q^1, \dots, Q^5, Y^2, \dots, Y^4]^T$  and taking into account the representation of flexible displacements (1)–(2) and constraints (3)–(6), the equations of the MS dynamics during the deployment of the boom can be obtained using the Lagrangian formalism and presented in the following general form:

$$M(\mathbf{X}, t) \ddot{\mathbf{X}} + D(\mathbf{X}, \dot{\mathbf{X}}, t) + C(\mathbf{X}, t) + \Phi_{\mathbf{X}}^T \Lambda = \mathbf{V}(t), \quad (7)$$

$$\Phi(\mathbf{X}) = \mathbf{0},$$

where  $M(\mathbf{X}, t)$  is the mass matrix;  $D(\mathbf{X}, \dot{\mathbf{X}}, t)$  is the vector containing gyroscopic and damping terms;  $C(\mathbf{X}, t)$  is the vector representing stiffness of system,  $\mathbf{V}(t)$  is the vector of non-conservative generalized forces caused by the action of the actuators and disturbances;  $\Lambda$  is the vector of Lagrange multipliers.

The damping matrix was constructed as proportional to the stiffness matrix.

**MS attitude control.** The control actions were synthesized without taking into account the flexibility of the MS. Using the new state vector  $\tilde{\mathbf{X}} = [x_1, x_2]^T = [Q^1, \dot{Q}^1]^T$ , the initial nonlinear system of equations (7) is transformed to an equivalent linear system [18]

$$\dot{x}_1 = x_2, \dot{x}_2 = U. \quad (8)$$

In equation (8), the quaternion is interpreted as control, and the control torque acting on the MS is calculated by the following transform:

$$T_u = 2J \left( q_0^1 \tilde{u} - u_0 q^1 - q^1 \times \tilde{u} \right) - \omega_0 J (\omega \times e_n) + \omega^1 \times J \omega^1, \quad (9)$$

where  $J$  is the MS inertia matrix,  $\omega^1$  is the vector of the absolute angular velocity of the MS in the platform fixed reference frame;  $\check{S}_0$  is the orbital angular velocity;  $e_n$  is the representation of the unit vector, which is normal to the orbital plane, in the BRF;  $u_0, \tilde{u}$  are the scalar and vector parts of the quaternion  $U$ , respectively.

The control torque includes feedforward and feedback terms:

$$T_u = T_u^f + T_u^b, U = U^f + U^b.$$

Here, the superscripts  $f$  and  $b$  denote the feedforward and feedback control, respectively.

The dynamics of the attitude error  $E$  can be described by the following equation

$$\ddot{E} = U^b,$$

This plant represents four uncoupled double integrators and can be stabilized by four proportional-derivative regulators as follows:

$$U^b = -k_p E - k_d \dot{E},$$

The gains of the regulators are selected using the Butterward distribution as follows:

$$k_p = \Omega^2, \quad k_d = 1.4\Omega,$$

where  $\Omega$  is the regulator bandwidth.

After finding the feedforward and feedback controls, the physically implementable control torque can be found using the transform (9).

**Simulation results.** The boom deployment was simulated using the following initial data:

*Rigid bodies.*

Mass and inertia matrix of the MS platform  $m^1 = 200$  kg and  $J^1 = \text{diag}(21.171, 21.211, 15.979)$  kg · m<sup>2</sup>, respectively;

Mass and inertia matrix of the stowed antenna  $m^5 = 7.406$  kg and  $J^5 = \text{diag}(0.503, 0.503, 0.073)$  kg · m<sup>2</sup>, respectively.

*Flexible bodies.*

Length of a single section of the boom is 1.227 m; the cross section of the boom is a tube with a diameter of 0.06 m and a wall thickness of 0.003 m; mass of a single section of the boom is 6 kg; Young's modulus 120 GPa; Poisson's ratio 0.3.

*Revolute joints.*

Static friction coefficient is 0.5; dynamic friction coefficient is 0.3; translational speed of sticking is 1e-4 m/s; maximum sticking deformation is 1e-5 m.

First, we consider the scenario of the boom deployment No. 1.

At the first stage, a constant control torque  $-2$  N is applied to the platform around the  $z$ -axis for a time interval of 10 s (Fig. 3). At this stage, the fastening of the boom to the MS platform is released and, together with the antenna, it begins a rotational motion around the joint 1 until the locking mechanism latches. After that, the MS is stabilized in its nominal orientation. At the moment when the joint latched, the angular velocity of the MS was about 0.6 rad/s.

At the second stage, a constant control torque  $-2$  N is applied to the platform around the  $x$ -axis also for a time interval of 10 s (Fig. 4) and the fastening of the first section of the boom is released and the second and third sections, together with the antenna, begin a rotational motion around the joint 2 until its fixation mechanism latches. After that, the satellite is also stabilized in its nominal orientation. The second joint latched at a MS angular velocity of about 0.2 rad/s.

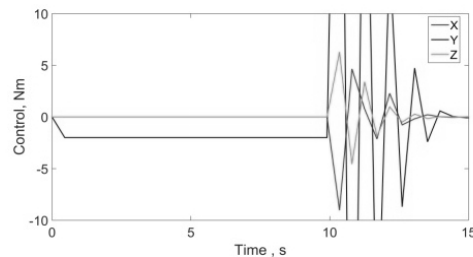


Fig. 3 – MS control torque variation during deployment stage 1 (scenario No 1)

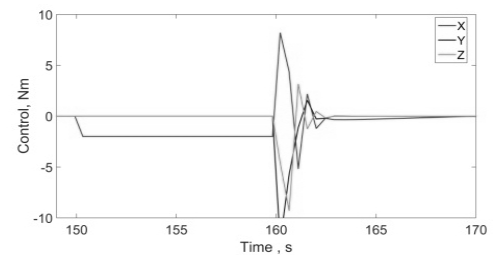


Fig. 4 – MS control torque variation during deployment stage 2 (scenario No 1)

At the final stage, a constant control torque of 2 N is applied to the platform around the  $x$ -axis for a time interval of 12 s and the fastening of the third section of the boom is released, and it, together with the antenna, begins a rotational motion around the joint 3 until its locking mechanism latches. After that, the satellite is also stabilized in its nominal orientation. At the moment when the joint latched, the angular velocity of the MS was about 0.1 rad/s.

Figures 6 shows the variation of the rotation angles of the joints. In the simulation, the stowed position of the boom corresponds to the angles of  $-90$  and  $180$  degrees for joint 1 and joints 2, 3, respectively. As can be seen from Fig. 6, all sections of the boom are fully deployed, and their joints are latched, however, as follows from Fig. 7, 8, the joints of the boom sections experience significant loads at the moment of joint latching (up to 300 Nm). In addition, Fig. 3– Fig.4 illustrate that when considered control laws are used, a large control torque is required to stabilize the MS after latching the joints. Therefore, for the practical implementation of this scenario, it is necessary to develop more advanced algorithms for damping angular velocities, taking into account the actuator constraints.

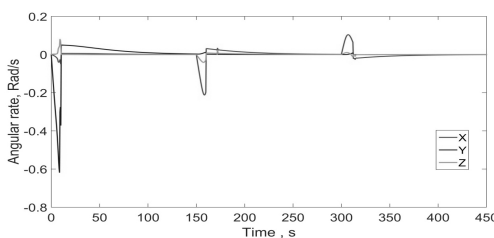


Fig. 5 – MS angular velocity variation (scenario No 1)

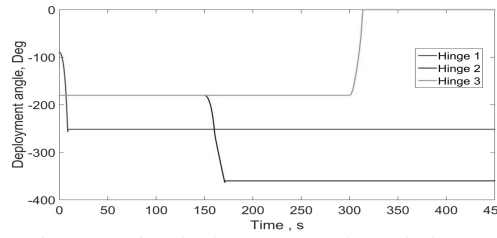


Fig. 6 – Joint deployment angle variation (scenario No 1)

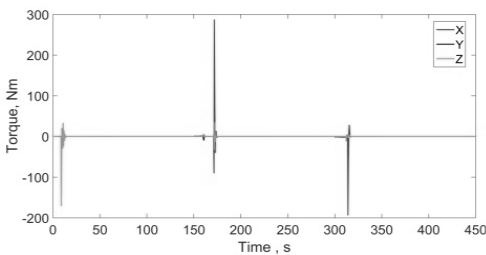


Fig. 7 – Torque variation in joint 1 (scenario No 1)

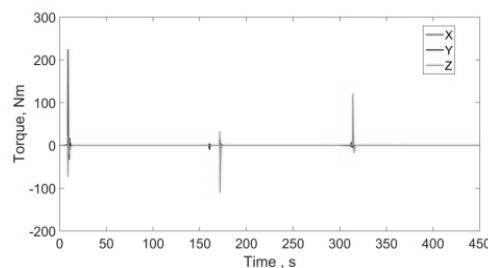


Fig. 8 – Torque variation in joint 2 (scenario No 1)

Let us consider deployment scenario No 2, in which the control system first provides the required angular velocity of the MS at each stage of the boom deployment. After the acquisition of the MS of the required angular velocity, the fasteners of the corresponding section of the boom are released and its deployment begins. At each deployment stage, the angular velocity of the MS is kept constant. The simulation results for such a scenario are shown in Fig. 9–Fig.12. This scenario makes it possible to provide the necessary centrifugal force by directly controlling the angular velocity of the MS and thus reduce the loads on the structure when the boom joints latch.



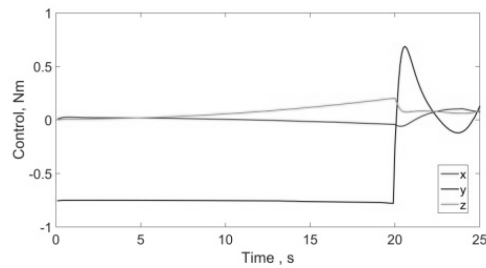


Fig. 9 – MS control torque variation during deployment stage 1 (scenario No 2)

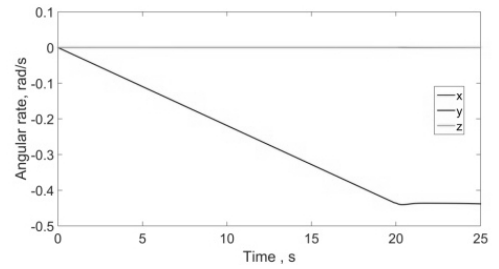


Fig. 10 – MS angular velocity variation during deployment stage 1 (scenario No 2)

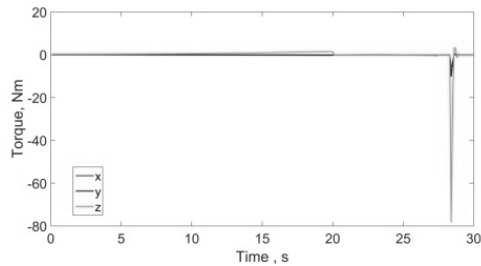


Fig. 11 – Torque variation in joint 1 during deployment stage 1 (scenario No 2)

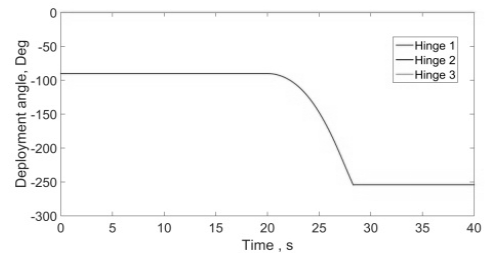


Fig. 12 – Joint deployment angle variation during deployment stage 1 (scenario No 2)

**Conclusion.** The article presents results of the simulations of centrifugal deployment of the three-section boom on an Earth observing minisatellite. The simulation results allow us to conclude that it is feasible to implement such a deployment strategy for a minisatellite, which can execute fast slew maneuvers about three axes of the body fixed reference frame. However, for practical implementation, additional research is required to design algorithms for controlling the attitude motion of the minisatellite, which will provide a guaranteed level of reliability of the boom deployment and joint latching with minimal loads on the structure. These issues may be the subject of further research.

1. . 2012. 3. . 85–97.
2. Duan B., Zhang Y., Du J. Large Deployable Satellite Antennas: Design Theory, Methods and Applications Springer Nature, 2020. 271 pp. <https://doi.org/10.1007/978-981-15-6033-0>
3. Alpatov A., Gusynin V., Belonozhko P. et.al. Shape control of large reflecting structures in space. 62nd International Astronautical Congress. 3–7 October. Cape Town. South Africa. 2011. Pp. 5642–5648.
4. Alpatov A., Gusynin V., Belonozhko P., Khoroshylov S., Fokov A. Configuration modeling of cable-stayed space reflectors. Proceeding of the 64nd International Astronautical Congress. Beijing. 2013. China. Pp. 5793–5799.
5. Li T.J., Zhang Y., Li T. Deployment dynamic analysis and control of hoop truss deployable antenna. Acta Aeronautica et Astronautica Sinica. 2009. Vol. 30, No.3. Pp.444–449.
6. Li T.J. Deployment analysis and control of deployable space antenna. Aerosp. Sci. Technol. 2012. Vol. 18, No 1. Pp. 42–47. <https://doi.org/10.1016/j.ast.2011.04.001>
7. Zhangn Y., B. Duan B., Li T.J. A controlled deployment method for flexible deployable space antennas. Acta Astronautica. 2012. Vol. 81, No 1. Pp.19–29. <https://doi.org/10.1016/j.actaastro.2012.05.033>
8. Lytal P., Renson M. Spacecraft common deployable boom hinge deploy and latching mechanisms. 44th Aerospace Mechanisms Symposium, 16-18 May, Cleveland, 2018. Pp.403–416.
9. Herbeck L., Leipold M., Sickinger C., Eiden M., Unckenbold W. Development and Test of Deployable Ultra-Lightweight CFRP-Booms for a Solar Sail. European Conference on Spacecraft Structures. Materials and Mechanical Testing, Nov. 28 –Dec. 1 2001, Noordwijk. The Netherlands, 2001. Pp.1–6.
10. Straubel M., Sinapius M., Langlois S. On-Ground Rigidised, Deployable Masts for Large Gossamer Space Structures. European Conference on Spacecraft Structures, Materials & Mechanical Testing. 15–17 Sep. 2009, Toulouse, France, 2009. Pp.1–7.
11. Straubel M., Zander M.E., Huhne C. Design and Sizing of the GOSSAMER Boom Deployment Concept. 3rd International Symposium on Solar Sailing. 11-13 Jun. 2013, Glasgow, Scotland, 2013. Pp.1–9.

12. *Sushko O., Medzmariashvili E., Tserodze S., et al.* Design and Analysis of Light-Weight Deployable Mesh Reflector Antenna for Small Multibeam SAR Satellite. EUSAR 2021: Proceedings of the European Conference on Synthetic Aperture Radar. 29 March – 01 April 2021, online, Pp. 421–423
13. *Sushko O., Medzmariashvili E., Filipenko F., et al.* Modified design of the deployable mesh reflector antenna for mini satellites. *CEAS Space J.* 2021. Vol. 13, No 4. Pp.533 – 542. <https://doi.org/10.1007/s12567-020-00346-0>
14. *Sullivan G., Blandino J., Hayes T., Amato Jr.T.* Boom Deployment Mechanism for CubeSats. AIAA SciTech Forum. 6-10 January, 2020, Orlando, FL. Pp.1–10. <https://doi.org/10.2514/6.2020-1672>
15. *Andión J., Pascual C.* Useful experiences in a series of deployable booms for CLUSTER satellites. Proceedings of the 9th European Space Mechanisms and Tribology Symposium. 19-21 Sep. 2001, Liège, Belgium. Pp.113 – 120.
16. *Gianfiglio G., Yorck M., Luhmann H.* Special features of the CLUSTER antenna and radial booms design, development and verification. The 29th Aerospace Mechanisms Symposium. 1 May, 1995, NASA Johnson Space Center, USA. P. 221 – 237.
17. *Shabana A.* Dynamics of Multibody Systems. Cambridge: Cambridge University Press, 2005. 374 pp. <https://doi.org/10.1017/CBO9780511610523>
18. *Yefimenko N.V.* Synthesis of Control Algorithms of the Spacecraft Spatial Reorientation with the Use of Dynamic Equations of a Solid Body Rotational Motion in Rodrigo-Hamilton Parameters. *Journal of Automation and Information Sciences.* 2015. Vol. 47, No. 6. Pp. 1–16. <https://doi.org/10.1615/JAutomatInfScien.v47.i6.10>

Received on 04.11.2021,  
in final form on 23.11.2021